



Solid state ^{13}C -NMR spectroscopy and XRD studies of commercial and pyrolytic carbon blacks

Hans Darmstadt^{a,b}, Christian Roy^{a,b,*}, Serge Kaliaguine^a, Guoying Xu^a,
Michèle Auger^c, Alain Tuel^d, Veda Ramaswamy^e

^aUniversité Laval, Département de génie chimique, Québec (Québec) Canada G1K 7P4

^bInstitut Pyrovac Inc., Parc technologique du Québec métropolitain, 333 rue Franquet, Sainte-Foy (Québec) Canada G1P 4C7

^cDépartement de chimie, CERSIM, Université Laval, Québec (Québec) Canada G1K 7P4

^dInstitut de Recherches sur la Catalyse, 2 Avenue Albert Einstein, F-69626 Villeurbanne, France

^eNational Chemical Laboratory, Pune 411 008, India

Received 3 May 1999; accepted 19 October 1999

Abstract

The bulk chemistry of commercial carbon blacks and carbon blacks obtained by vacuum pyrolysis (CB_p) of used tires was investigated by ^{13}C -NMR spectroscopy with and without magic angle spinning of the sample. Two different kinds of carbon atoms can be distinguished: Graphite like carbon atoms in poly-condensed aromatic rings and carbon atoms in a less ordered environment. Commercial carbon blacks and CB_p obtained under different pyrolysis conditions have practically the same concentrations of the different types of carbon atoms in the bulk, whereas earlier ESCA and SIMS investigations have shown that the surface chemistry of CB_p is different from commercial carbon blacks and depends strongly on the pyrolysis conditions. Thus, during the pyrolysis only the carbon black surface chemistry is changed. The carbon black bulk structure was also studied by X-ray diffraction. The XRD results, including the radial distribution function (RDF) indicated, in agreement with the NMR results, that the bulk structure of commercial carbon blacks and of CB_p are similar. © 2000 Elsevier Science Ltd. All rights reserved.

Keywords: A. Carbon black; B. Pyrolysis; C. Nuclear magnetic resonance (NMR), X-ray diffraction; D. Chemical structure

1. Introduction

The huge piles of scrap tires are usually considered as waste material. In the USA approximately 63% of the scrap tires are dumped in landfills and 23% are incinerated [1]. These treatments cannot be considered environmentally friendly. During incineration of tires, for example, carcinogenic polynuclear aromatic hydrocarbons are produced [2]. Vacuum pyrolysis offers an environmentally friendly way to transform scrap tires into useful products. Pyrolytic oil and pyrolytic carbon black (CB_p) are the principal products of this process [3]. The economy of the tire pyrolysis process strongly depends on the quality of the CB_p , i.e. its ability to be used in high value commercial applications (e.g. as reinforcing filler in polymers). The

CB_p consists of the recovered carbon black filler, inorganic tire components (e.g. ZnS and ZnO [4]) and carbonaceous deposits that may have been formed during the pyrolysis. Carbonaceous deposits are defined here as chemically bound (mostly aromatic) hydrocarbons on the carbon black surface. Such deposits can be formed from hydrocarbons adsorbed on the carbon black surface. Their presence on the carbon black and on inorganic CB_p components was confirmed by surface spectroscopic methods such as ESCA and SIMS [5,6] and scanning electron microscopy [4].

By means of a mass balance it is possible to make a coarse estimate of the amount of carbonaceous deposits. Tires contain approximately 25–30% of carbon black and 4% of inorganic components (e.g. ZnO and S) [1,7] on a steel-free basis. The inorganic tire components usually end up in the CB_p . Thus, if no carbonaceous deposits are formed, tire pyrolysis should yield approximately 29–34% CB_p . Higher CB_p yields indicate the formation of carbonaceous deposits during the pyrolysis. Tire pyrolysis can

*Corresponding author. Tel.: +1-418-656-2131 Ext. 6931; fax: +1-418-656-2091.

E-mail address: croy@gch.ulaval.ca (C. Roy).

be performed at atmospheric [8–12] or at reduced pressure [3,13]. Yields of 40% [14] and 52% CB_p [15], respectively, have been reported for atmospheric tire pyrolysis at 500°C. These high CB_p yields suggest that considerable amounts of carbonaceous deposits are formed during atmospheric tire pyrolysis. The situation is different for tire pyrolysis at reduced pressure. In the authors' laboratory the CB_p yields for tire pyrolysis at 500°C ranged between 30 and 34%. This suggests that during pyrolysis at reduced pressure no or only small amounts of carbonaceous deposits were formed. The difference between pyrolysis at atmospheric and reduced pressure may be explained by the different concentrations of hydrocarbons in the gas phase. During the pyrolysis the atmosphere in the reactor consists of the hydrocarbons formed from the decomposing elastomer. These hydrocarbons may adsorb on the carbon black surface, polymerise there and finally form carbonaceous deposits. These reactions will be limited if the hydrocarbon concentration in the gas phase is reduced, for example by reducing the pressure in the reactor. A correlation between the amount of carbonaceous deposits on the CB_p surface and the pyrolysis pressure was indeed observed [5,6]. The residence time of gases is directly proportional to the pressure. Due to the low residence time during the vacuum pyrolysis process, hydrocarbons formed from the decomposing elastomer do not have "the time" to form precursors of carbonaceous deposits in the gas phase.

The above mentioned mass balance indicates that CB_p from pyrolysis at reduced pressure contains no or only small amounts of carbonaceous deposits. However, such a mass balance only allows a rough estimate of the amount of carbonaceous deposits. First, the feedstock consists of a mixture of different used tires with different concentrations of carbon black. Second, even if the carbon black content of the new tires is known, the composition changes during their use (e.g. through abrasion of the tire tread). Thus, a direct measure of the amount of carbonaceous deposits on the CB_p is desirable. Two different methods were employed in this work to characterise the bulk of CB_p in comparison with commercial rubber grade carbon blacks. The bulk chemistry was studied by ^{13}C -NMR, whereas X-ray diffraction data were used to calculate the dimension of graphitic domains and the radial electron distribution function.

^{13}C -NMR spectra of solid carbonaceous solids usually exhibit broad lines and the distinction of different carbon types is not easy. The most important broadening mechanism in the ^{13}C -NMR solid state experiment of polycrystalline samples is the Chemical Shift Anisotropy (CSA). The CSA can be removed by magic angle spinning (MAS) and as a result the line widths are considerably reduced. However, the averaging of the different chemical shift tensors leads to a loss of information. For example, the chemical shift tensors of carbons in condensed aromatic compounds and of carbons in one-ring aromatic compounds are quite different, whereas the average chemi-

cal shifts observed in the MAS spectrum are usually too close to be separated in spectra of solid samples. Chemical shift tensors of a variety of hydrocarbons were listed by Duncan [16]. The chemical shift tensors for similar types of carbon (e.g. aromatic carbons which are bound only to other aromatic carbons) differ only a little. It is, therefore, possible to fit experimental spectra to "standard" peaks of different carbon types. This approach was used by Wemmer et al. [17], Orendt et al. [18] and Sethi et al. [19] to analyse coal and other carbon samples. The carbon atoms were divided by Wemmer et al. [17] into four types: Aliphatic carbons, alkoxy carbons, aromatic carbons bound only to other aromatic carbons and aromatic carbons bound to aliphatic substituents or hydrogen. Orendt and Sethi used the same classification. However, they differentiated further between aromatic carbon atoms with aliphatic substituents and those bound to hydrogen.

Graphene layers are the basic building block of carbon black particles and these layers exhibit numerous distortions and discontinuities [20]. Some regions, however, have a more regular, graphite-like arrangement. The dimensions of these graphitic domains are characterised by the average stacking height of the parallel layers in the "c" direction (L_c) and by the average diameter of the parallel layers in the "ab" plane (L_a). These two dimensions can be determined by X-ray diffraction. If the carbonaceous deposits on the CB_p contain polyaromatic compounds with a lower order as compared to the commercial carbon black initially present in the tire the average dimension of the "crystalline" domains in the CB_p should be smaller than in the commercial carbon black.

The radial electron distribution function (RDF) of commercial carbon blacks has been measured by different groups [21–23]. As already mentioned, in carbon black the carbon atoms are present in graphite-like layers. However, there is no long range three-dimensional order as in graphite [20]. The presence of carbonaceous deposits on the CB_p should influence their RDF. The average size of a system consisting of condensed aromatic rings, for example, can also be determined from RDF [24,25]. Since the size of the aromatic system in carbonaceous deposits is much smaller than in the carbon black, this can be tedious applied to detect carbonaceous deposits in the CB_p . Carbonaceous deposits can also be identified if they contain aliphatic domains with sp^3 hybridised carbon atoms because these atoms have different numbers of neighbours from atoms in carbon black. RDF was also found sensitive enough to determine the vitrinite concentrations in coals [26].

2. Experimental details

2.1. Materials

The CB_p samples were obtained by vacuum pyrolysis of

tire parts from the sidewall of cross-ply tires at temperatures and total pressures ranging from 420 to 700°C and 0.3 to 20 kPa, respectively. A detailed description of the feedstock, the reaction conditions and the reactor has already been published [27,28]. Four grades of commercial rubber grade carbon blacks were investigated for comparison. The grades N539, N660 and N774 were chosen because these three grades are used in the sidewall of tires, whereas the grade N110 is used in the tread [7]. Their surface areas are similar to those of CB_p and their ESCA C_{1s} spectra are representative for commercial rubber grade carbon blacks [5]. The graphite powder used for the NMR experiments was purchased from Fisher Scientific Canada, Grade #38.

2.2. Characterisation

2.2.1. Static ¹³C-NMR experiments

The ¹³C-NMR experiments were performed with an ASX 300 spectrometer from Bruker Canada Ltd., Milton, Ontario, Canada (Université Laval) at a carbon frequency of 75.42 MHz. The spectra were acquired with a Hahn echo sequence and high power proton decoupling during data acquisition. The 90° pulse width was 4.5 μs and the recycle delay was 20 s. A longer recycle delay did not increase the intensity of the spectra. All free induction decays were subjected to Fourier transformation and a 500 Hz line broadening was applied to all spectra. The chemical shifts δ , expressed in parts per million [ppm], were referenced relative to the signal of tetramethylsilane (TMS) at $\delta_c = 0$ ppm. For every spectrum 4000 scans were added. The experimental spectra were fitted to theoretical static spectra of different carbon types using the equations given in [29] with an additional Gauss–Lorentz line broadening. The fitting program allowed the variation of the peak intensity, the three chemical shift tensor components (δ_{11} , δ_{22} and δ_{33}), the width of the Gauss–Lorentz broadening function (ΔB) and the Gauss–Lorentz mixing ratio (gl).

2.2.2. ¹³C-MAS–NMR experiments

Single pulse ¹³C-MAS–NMR spectra were recorded with a MSL 300 spectrometer from Bruker, Rheinstetten, Germany (CNRS, Villeurbanne) operating at a carbon frequency of 75.47 MHz and a spinning frequency of 4 kHz. The 90° pulse width was 7 μs and high power proton decoupling was performed during recording of the spectra. The recycle delay was 20 s and 4000 scans were added for every spectrum.

2.2.3. X-ray diffraction experiments

The diffraction experiments were performed with a Rigaku, Tokyo, Japan model D Max III VC diffractometer (NCL, Pune) using CuK α radiation. The dimensions of the domains with a graphite-like order were calculated using the (002) and (11) reflections and the Scherrer equation,

respectively [30]. The calculation of the RDF followed the procedure given in [30].

3. Results and discussion

3.1. ¹³C-NMR spectra

The static ¹³C-NMR spectra of two commercial carbon black samples (N539 and N774) and the CB_p samples were fitted to two peaks (Figs. 1 and 2). The principal tensor components of the two peaks in the spectra of the commercial carbon blacks are very similar (Table 1) and close to those of the different CB_p (Table 2). These tensor components represent the shielding constants along the three principal axes in a molecule-fixed system. The most intense peak (C₁) had average tensor components ($\delta_{11} = 186.5$ ppm, $\delta_{22} = 183.3$ ppm, $\delta_{33} = 9.9$ ppm) which are typical for carbon atoms in condensed aromatic compounds [16] and which are close to the tensor components of graphite atoms ($\delta_{11} = \delta_{22} = 178$ ppm, $\delta_{33} = 0$ ppm) [31]. An assignment of this peak to graphite-like carbon atoms in condensed aromatic compounds is reasonable since individual graphitic layers are the basic building block of carbon black particles [20] and the XRD spectra of the two commercial carbon blacks and the CB_p also show the reflections of graphite (Fig. 3). These reflections are very broad, indicating that the graphitic domains are relatively small. The average stacking height (L_c) and the average

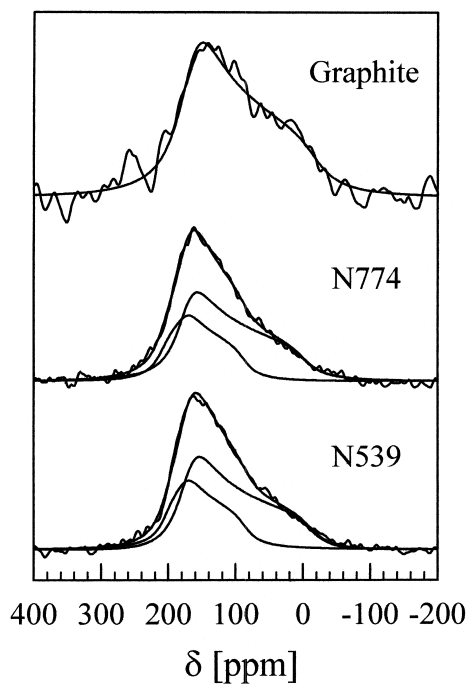


Fig. 1. ¹³C-NMR spectra of commercial carbon blacks and graphite.

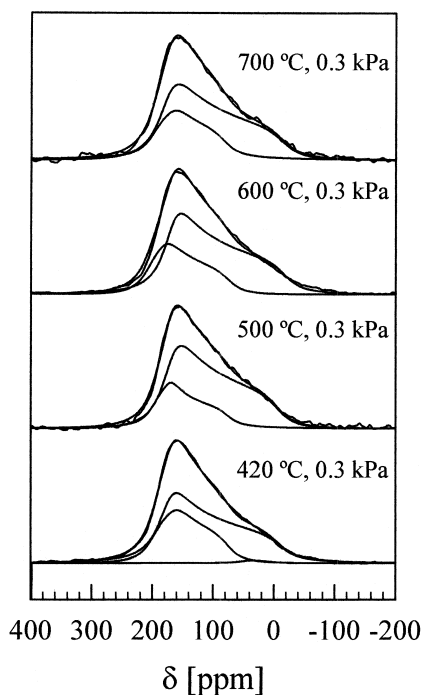


Fig. 2. ^{13}C -NMR spectra of pyrolytic carbon blacks.

diameter (L_a) of the parallel graphite-like layers in the commercial carbon blacks studied here are between 13 and 16 and 17–20 Å, respectively (Table 3).

The second peak (C_2) has tensor components which are close to those of phenolic carbon atoms [16]. However, since the bulk oxygen concentration of commercial carbon blacks and CB_p is small [4] (<4 wt. %), this peak cannot be assigned to phenolic carbon atoms. An assignment of the C_2 peak to carbons bound to other elements was also ruled out, because of the low concentration of other non-carbon elements in CB_p . In carbon blacks the graphitic layers exhibit numerous distortions and discontinuities [20]. The electronic environment, and therefore also, the

chemical shift tensor components, of carbons in these distorted regions of the graphitic layers will certainly differ from the carbons in the well-ordered regions. For example in turbostratic graphite the tensor components of the carbons ($\delta_{11}=251$ ppm, $\delta_{22}=\delta_{33}=20$ ppm) [32] differ considerably from those of graphite (see above). Consequently, the C_2 peak was assigned to carbons in disordered regions of the graphene layers.

As with the static spectra, the ^{13}C -MAS-NMR spectra of commercial carbon blacks and of the CB_p were also similar. The ^{13}C -MAS-NMR spectra of the two commercial carbon blacks and the CB_p showed a broad peak with a chemical shift of approximately 130 ppm and a broad shoulder at approximately 170 ppm. As an example, the spectrum for the CB_p sample obtained at 500°C and 0.3 kPa is presented in Fig. 4. The position and intensity ratio of the two signals in the MAS spectrum support the fit results of the static spectra, since the position of the signals in the ^{13}C -MAS-NMR spectra correspond to the average of the three chemical tensor components [$\delta_{\text{avg.}} = 1/3 \cdot (\delta_{11} + \delta_{22} + \delta_{33})$] of the static spectra. This comparison can be made from the results presented in Tables 1 and 2, where $\delta_{\text{avg.}}$ of the two peaks are listed. In all cases the differences between $\delta_{\text{avg.}}$ of the static spectra and the position of the two signals in the MAS spectra are smaller than 10 ppm.

In the static spectrum of the CB_p sample which was obtained at a pyrolysis temperature of 420°C, a very small third peak (C_3) was detected (Table 2). In this CB_p sample small amounts of not completely decomposed elastomer were detected by scanning electron microscopy (SEM) [4]. Accordingly, the C_3 peak was assigned to aliphatic carbons since it also has tensor components typical for aliphatic carbons [16]. Pyrolysis temperatures of 500°C and higher ensured the complete decomposition of the elastomer and neither incompletely decomposed elastomer nor a C_3 peak was detected by SEM and ^{13}C -NMR spectroscopy, respectively.

The absence or very small concentration of aliphatic carbon atoms or other carbon atoms bound to hydrogen in

Table 1
Relative intensities and tensor components of different carbon types in commercial carbon blacks and graphite

Commercial carbon black	Type of carbon atom											
	Graphite-like carbon atoms						Carbon atoms in disordered environment					
	Grade	Area [%]	Tensor components [ppm]				Width ^a [ppm]	Area [%]	Tensor components [ppm]			
δ_{11}			δ_{22}	δ_{33}	$\delta_{\text{avg.}}$	δ_{11}			δ_{22}	δ_{33}	$\delta_{\text{avg.}}$	
N 539	63	186.4	180.1	4.8	123.8	25.5	37	217.3	186.0	102.3	168.5	18.1
N 774	67	186.7	186.4	15.0	129.4	25.1	33	224.9	186.0	103.0	171.3	18.0
Graphite ^b	100	179.8	179.8	-1.0	119.5	30.5	-	-	-	-	-	-

^a Gauss-Lorentz line broadening.

^b Literature data: $\delta_{11}=\delta_{22}=178$ ppm, $\delta_{33}=0$ ppm [31].

Table 2
Relative intensities and tensor components of different carbon types in pyrolytic carbon blacks

Pyrolysis conditions		Carbon type											
		Graphite-like carbon atoms						Carbon atoms in disordered environment					
T [°C]	P [kPa]	Area [%]	Tensor components [ppm]				Width [ppm]	Area [%]	Tensor components [ppm]				Width [ppm]
			δ_{11}	δ_{22}	δ_{33}	$\delta_{avg.}$			δ_{11}	δ_{22}	δ_{33}	$\delta_{avg.}$	
420 ^a	0.3	64.4	197.3	181.6	4.6	127.8	23.7	34.6	213.6	176.0	90.2	159.9	20.0
500	0.3	69.2	183.0	177.6	4.1	121.6	26.3	30.8	210.3	183.8	88.9	161.0	15.6
600	0.3	66.5	185.1	179.2	-1.7	120.9	27.3	33.5	220.8	191.2	90.8	167.6	19.2
700	0.3	66.2	193.8	184.8	1.8	126.8	26.3	33.7	213.8	178.6	95.3	162.6	21.0
500	10.0	67.0	199.8	191.4	-4.3	129.0	27.2	33.0	227.0	190.0	102.1	173.0	17.3
500	20.0	65.4	194.8	181.6	4.6	127.0	25.6	34.5	217.3	174.9	84.3	158.8	18.9

^a A third peak was detected for aliphatic carbon: Area 1%; δ_{11} 49.9 ppm; δ_{22} 39.7 ppm δ_{33} 9.5 ppm

these CB_p samples was also confirmed by the observation that the cross-polarised ^{13}C -MAS-NMR spectra of these samples showed hardly any signal (spectra not shown).

The relative areas of the C_1 and C_2 peaks were very similar for the CB_p from different pyrolysis conditions (Table 2), suggesting that the pyrolysis temperature and pressure had no or very little influence on the bulk composition of the CB_p (not considering the inorganic CB_p portion). The relative areas of the two peaks in the spectra of the two commercial carbon blacks were also

very close to those of the CB_p . The C_1 peaks in the spectra of the two commercial carbon blacks were either slightly smaller (N539) or slightly more intense (N774) than in the spectra of the CB_p (Table 1). Since tires contain different commercial carbon blacks (e.g. N539 and N660 in the carcass (tire structure except the sidewall and tread) and N765 and N774 in the tire sidewall [7]) the recovered CB_p is a mixture of the different commercial carbon blacks. Therefore, it can be concluded that the bulk of the carbon black filler is not or only very little changed during the tire pyrolysis.

3.2. X-ray diffraction

As already mentioned above CB_p contain inorganic components. The CB_p diffractograms showed, therefore, signals of these components. Since we were only interested in the structure of the carbon portion of the CB_p the

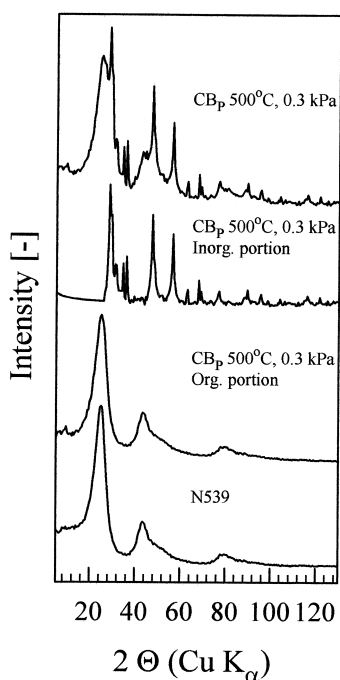


Fig. 3. Diffractograms of pyrolytic carbon black @ 500°C, 0.3 kPa (before and after correction for inorganic CB_p components) and of commercial carbon blacks.

Table 3
Dimensions of graphitic domains in commercial and pyrolytic carbon blacks as derived from XRD

Commercial black		L_s	L_g
Grade	Surface area [m ² /g]	[Å]	[Å]
N110	145	13.3	17.0
N539	43	15.2	18.1
N660	36	16.0	20.0
N774	29	16.2	20.1
Pyrolytic carbon black, pyrolysis conditions		L_c	L_a
T [°C]	P [kPa]	[Å]	[Å]
420	0.3	15.8	19.2
500	0.3	15.8	19.2
500	10.0	15.8	19.2
500	20.0	15.8	19.2
600	0.3	15.8	19.2
700	0.3	15.8	19.2
700	10.0	15.8	19.2
700	20.0	15.8	19.2

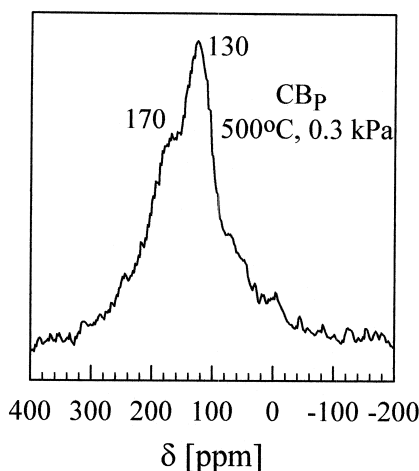


Fig. 4. ^{13}C -MAS-NMR spectrum of pyrolytic carbon black @ 500°C, 0.3 kPa.

contribution of the inorganic components was subtracted from the CB_p diffractograms. This is shown in Fig. 3 for the CB_p sample obtained at a temperature and pressure of 500°C and 0.3 kPa, respectively. The upper spectrum is the experimental diffractogram of the CB_p . This CB_p contains a mixture of different Zn compounds (ZnO, α -ZnS and β -ZnS, [4]). The combined diffractogram of these inorganic compounds is shown below the experimental diffractogram. By subtraction the diffractogram of the carbon portion of the CB_p was obtained. The diffractograms of the carbon portion of the different CB_p samples studied here and the diffractograms of the commercial carbon blacks were very similar, indicating that the carbon portion of the CB_p did not contain significant amounts of carbonaceous deposits.

XRD investigations of commercial carbon blacks showed that the dimensions of the “crystalline” regions, especially L_c , increase in general with decreasing specific surface area, or increasing radius of the spherical primary carbon black particles [20]. This may be related to the radius of curvature, since a larger radius of the carbon

black particle should allow a more “undisturbed” arrangement of the graphene layers in an ordered graphite-like structure. For the four commercial carbon black samples studied here L_c and L_a increased with decreasing specific surface area (Table 3). For all the CB_p samples, L_c and L_a were identical. The values of L_c and L_a were between the corresponding values of the medium and low surface area commercial blacks, which are used in tire side walls. These findings suggest that in the different CB_p , only very small concentrations of carbonaceous deposits were present.

3.3. XRD – radial distribution function

The RDF of four commercial carbon black grades showed signals at approximately 1.5, 2.6, 3.65, 4.2 and 5.1 Å, respectively (Table 4). The signal at approximately 3.65 Å was for most of the samples only resolved as a shoulder. As an example the RDF of the commercial carbon black N539 is shown in Fig. 5. The RDF observed for the commercial carbon blacks in this work is in good agreement with the RDF of carbon blacks observed by Warren [21] and other authors [23]. For comparison, the theoretical values for distances and numbers of neighbours of a carbon atom in a single layer of graphite are also given in Table 4. All signals in the RDF plot of the commercial blacks can be explained by carbon atoms in the same single graphene layer (Fig. 6). For the atoms at a distance of 2.46 and 2.84 Å only one peak in the RDF plot at approximately 2.6 Å was found (Fig. 5). No signals of carbon atoms in adjunct graphene layers were found in the RDF. The number of approximately three and nine neighbours calculated for the first two RDF signals is also to be expected for a graphite layer.

The RDF plots calculated from the diffractograms of the carbon portion of the CB_p were very similar (Fig. 5). Also the number of neighbours and their distances in the carbon portion of the CB_p was practically the same as for the commercial carbon blacks (Table 5). The fact that both the commercial blacks and CB_p RDF curves yield distances and numbers of neighbours which are essentially the ones

Table 4
Interatomic distances (d) and number of neighbours (N) in commercial carbon blacks as determined from RDF data

Sample	d [Å] (N)				
Single graphite layer	1.42 (3.0)	2.46 (3.0)	3.75 (6.0)	4.25 (6.0)	4.92 (6.0)
Ref. [21]	–	2.84 (6.0)	–	–	5.11 (6.0)
Commercial black					
Cabot, Ref. [21]	1.50 (3.2)	2.70 (10.2)	4.05	–	5.15
Carbofrance, Ref. [23]	1.39 (~3)	2.55 (~11)	4.10	–	5.00
N 115	1.50 (2.5)	2.59 (9.4)	3.61	4.23	5.05
N 539	1.51 (2.8)	2.64 (10.1)	~3.65 ^a	4.22	5.07
N 660	1.50 (2.9)	2.63 (9.9)	~3.65 ^a	4.23	5.08
N 774	1.50 (2.8)	2.59 (9.7)	3.65	4.23	5.06

^a Shoulder

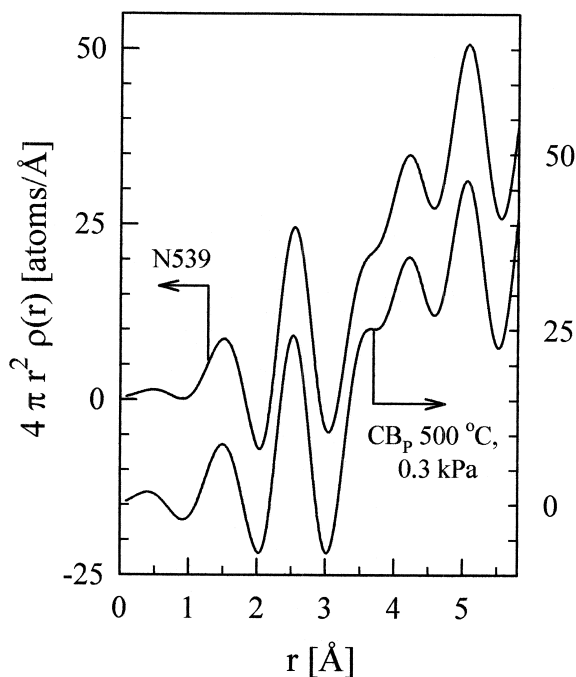


Fig. 5. Radial distribution function of commercial carbon black N539 and of the carbon portion of pyrolytic carbon black @ 500°C, 0.3 kPa.

of graphite monolayers (Fig. 6 and Tables 4 and 5) suggests that the graphene layers within the same graphitic domain are not arranged in a crystal-like structure. Although the distance between the layers in carbon black is known to be 3.6–3.7 Å, the location of the neighbouring carbon atoms in the adjacent layers must be randomly yielding a random distribution of carbon–carbon distances, which is in agreement with the accepted turbostratic structure of carbon blacks. The RDF results indicate again that no significant amounts of carbonaceous deposits were formed during the tire pyrolysis.

However, the pyrolysis conditions have an important influence on the surface chemistry of the CB_p . Earlier surface spectroscopic investigations of the same CB_p samples showed that deposits of pyrolytic carbon, consisting mostly of small aromatic compounds, are formed on the surface of CB_p during the pyrolysis [5,6]. These deposits originate from hydrocarbons adsorbed on the CB_p surface. Pyrolytic carbon deposition increases with increasing pyrolysis pressures and decreasing pyrolysis temperatures. The absence of a peak of carbons in small aromatic compounds in the ^{13}C -NMR spectra of CB_p , from pyrolysis temperatures at 500°C or higher temperatures, suggests that the pyrolytic carbon deposits are limited to the surface and make up only a very small part of the total carbon.

The observation that the bulk of commercial carbon

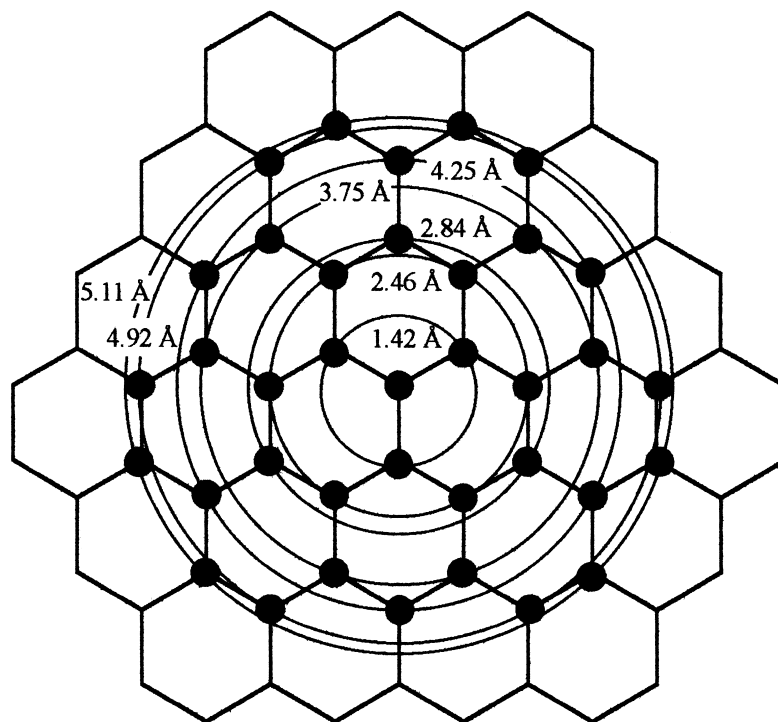


Fig. 6. Number of neighbours and their distances in a single layer of graphite.

Table 5

Interatomic distances and number of neighbours in pyrolytic carbon blacks (carbon portion) as determined from RDF data

Pyrolytic carbon black pyrolysis conditions		d [Å] (N)				
T [°C]	P [kPa]					
420	0.3	1.49 (2.9)	2.60 (9.8)	3.65 ^a	4.23	5.06
500	0.3	1.50 (2.9)	2.61 (9.9)	3.61	4.23	5.06
500	10.0	1.51 (2.8)	2.59 (9.8)	3.61	4.22	5.07
500	20.0	1.50 (2.8)	2.58 (9.7)	3.61	4.22	5.06
600	0.3	1.50 (2.9)	2.60 (9.8)	3.65 ^a	4.23	5.08
700	0.3	1.50 (2.9)	2.58 (9.6)	3.65 ^a	4.23	5.09
700	10.0	1.51 (2.8)	2.59 (9.7)	3.61	4.22	5.08
700	20.0	1.50 (2.9)	2.60 (9.7)	3.61	4.22	5.07

^a Shoulder.

blacks and CB_p have virtually the same chemical nature is very important for the application of CB_p. As shown previously, the two most important differences between commercial carbon blacks and CB_p are the deposition of pyrolytic carbon on the CB_p surface and the high concentration of inorganic compounds in CB_p [4–6]. Since these two differences can be reduced by a proper choice of the pyrolysis conditions [5,6,33] and a demineralisation treatment [34], respectively, vacuum pyrolysis has the potential to produce CB_p that is close in its properties to commercial carbon black.

The surface activity of CB_p was studied in a previous paper [35] by inverse gas chromatography (IGC). It is known that the IGC results correlate well with the mechanical properties of carbon black reinforced polymers [36]. The surface activity of CB_p was found to be approximately one third smaller as compared to the commercial carbon blacks initially present in polymer [35]. Therefore, a substitution of low and medium surface area commercial carbon black by high surface area CB_p should be technically possible for certain polymer applications. Work is underway in this laboratory to produce CB_p reinforced elastomers.

4. Conclusion

The bulk of the commercial carbon blacks N539 and N774 consists of approximately two thirds of graphite-like carbons in condensed aromatic compounds and of approximately one third of carbon in a less ordered environment. During pyrolysis of used tires at 500°C or higher temperatures at pressures below 20 kPa only minor amounts of carbonaceous deposits are formed on the surface of the CB_p particles. Thus, tire pyrolysis at reduced pressure yields CB_p which have a bulk chemical nature very similar to that of commercial carbon blacks. Variation of the pyrolysis temperature and pressure from 500 to 700°C and 0.3 to 20 kPa, respectively, does not change the bulk of the CB_p. The deposition of pyrolytic carbon, observed earlier

by surface spectroscopic methods, is limited to the surface of the CB_p, the concentration of pyrolytic carbon in the bulk is very small. Therefore, a substitution of commercial carbon black by CB_p for certain applications should be technically possible.

Acknowledgements

This research was supported by the Natural Sciences and Engineering Research Council of Canada (Ottawa), the Fonds pour la Formation de Chercheurs et l'Aide de la Recherche (Québec), the Ministère des Affaires Internationales et des Communautés Culturelles and Institut Pyrovac Inc. (Québec). Cabot (Canada) and Columbian Chemicals (Canada) provided the commercial carbon samples, for which the authors are grateful.

References

- [1] Schnecko H. Kautsch, Gummi Kunstst 1994;47:885.
- [2] Levendis YA, Atal A, Carlson J, Dunayevskiy Y, Vouros P. Environ Sci Technol 1996;30:2742.
- [3] Roy C, Labrecque B, de Caumia B. Resour Conserv Recycl 1990;4:203.
- [4] Darmstadt H, Roy C, Kaliaguine S. Kautschuk, Gummi und Kunststoffe 1994;47:891.
- [5] Darmstadt H, Roy C, Kaliaguine S. Carbon 1994;32:1399.
- [6] Darmstadt H, Roy C, Kaliaguine S. Carbon 1995;33:1449.
- [7] Waddell WH, Bhakuni RS, Barbin RS, Sandstrom PH. In: Ohm RF, editor, The vanderbilt rubber handbook, 13th ed., Norwalk, CT, USA: R.T. Vanderbilt Company, Inc, 1990, p. 596.
- [8] Schnecko H. Kautschuk, Gummi und Kunststoffe 1974;27:526.
- [9] Schnecko H. Chemie-Ingenieur-Technik 1976;48:443.
- [10] Williams PT, Besler S, Taylor DT. Fuel 1990;69:1474.
- [11] Williams PT, Taylor DT. In: Ferrero GL, Maniatis K, Buekens A, Bridgwater AV, editors, Pyrolysis and gasifica-

- tion, London, UK: Elsevier Applied Science, 1989, pp. 486–91.
- [12] Cypres R, Bettens B. In: Ferrero GL, Maniatis K, Buekens A, Bridgwater AV, editors, Pyrolysis and gasification, London, UK: Elsevier Applied Science, 1989, p. 209.
- [13] Roy C, Unsworth J. In: Ferrero GL, Maniatis K, Buekens A, Bridgwater AV, editors, Pyrolysis and gasification, London, UK: Elsevier Applied Science, 1989, p. 180.
- [14] Kawakami S, Inoue K, Tanaka H, Sakai T. In: Jones JL, Radding SB, editors, Thermal conversion of solid wastes and biomass, Vol. 130, Washington DC: American Chemical Society Symposium Series, 1980, p. 557.
- [15] Fader J. In: Autorecycle '94, Dearborn, Michigan, November 8–9, 1994, Paper presented.
- [16] Duncan TM. In: A compilation of chemical shift anisotropies, Chicago, USA: The Farragut Press, 1990, pp. C–1.
- [17] Wemmer DE, Pines A, Whitehurst DD. Philosophical Transactions of the Royal Society of London, Series A 1981;300:15.
- [18] Orendt AM, Solum MS, Sethi NK, Hughes CD, Pugmire RJ, Grant DM. In: Botto RE, Sanada Y, editors, Magnetic resonance of carbonaceous solids, advances in chemistry series, Vol. 229, Washington, USA: American Chemical Society, 1993, p. 419.
- [19] Sethi NK, Pugmire RJ, Facelli RJ, Grant DM. Anal Chem 1988;60:1574.
- [20] Hess WH, Herd CR. In: Donnet J-B, Bansal RC, Wang M-J, editors, Carbon black, 2nd ed., New York, USA: Marcel Dekker Inc, 1993, p. 89.
- [21] Warren BE. J Chem Phys 1934;2:551.
- [22] Krzton H, Niewiara M. Physica Scripta 1995;T57:98.
- [23] Oudet F, Vélux A. Analysis 1991;19:311.
- [24] Wertz DL, Bissell M. Adv X-ray Anal 1994;37:491.
- [25] Nelson JB. Fuel 1954;33:381.
- [26] Burrigato F, Caminiti R, Ferraro M, Gelli J, Sadun C. Fuel 1997;76:887.
- [27] Rastegar A. M.Sc. thesis, Québec, QC, Canada: Université Laval, 1989.
- [28] Roy C, Rastegar A, Kaliaguine S, Darmstadt H, Tochev V. Plast Rubber Composites Applic 1995;23:21.
- [29] Mehring M. In: Principles of high resolution NMR in solids, 2nd ed., Berlin, Germany: Springer-Verlag, 1983, p. 25.
- [30] Klug HP, Alexander LE. X-ray diffraction procedures for polycrystalline and amorphous materials, New York, USA: John Wiley & Sons, 1974, p. 791.
- [31] Resing HA, Weber DC, Anderson M, Miller GR, Moran M, Poranski CF, Mattix L. Polymer Preprints 1982;23:101.
- [32] Duncan TM, Winslow P, Bell AT. J Catal 1985;93:1.
- [33] Sahouli B, Brouers F, Blacher S, Darmstadt H, Roy C, Kaliaguine S. Fuel 1996;75:1244.
- [34] Chaala A, Darmstadt H, Roy C. Fuel Process Tech 1996;46:1.
- [35] Darmstadt H, Roy C, Kaliaguine S, Cormier H. Rubber Chem Tech 1997;70:759.
- [36] Donnet JB, Lansinger CM. Kautschuk, Gummi und Kunststoffe 1992;45:459.